Characterizing the Rate of Spread of Wildfires in Emerging Fire Environments of Northwestern Europe

Adrián Cardíl[1,2,3*], Mario Tapia[1,3*], Santiago Monedero[1], Kerryn Little[4], Cathelijne R. Stoof[5], Tomas Quiñones[1], Joaquin Ramirez[1], Sergio de-Miguel[2,3]

[1]Tecnosylva, S.L Parque Tecnológico de León, 24004 León, Spain
[2]Joint Research Unit CTFC - AGROTECNIO - CERCA, 25280 Solsona, Spain
[3]Department of Crop and Forest Sciences, University of Lleida, 25198 Lleida, Spain
[4]School of Geography, Earth and Environmental Sciences, University of Birmingham, Birmingham, UK
[5]Department of Environmental Sciences, Wageningen University, PO box 47, 6700 AA Wageningen, The Netherlands

Correspondence to: Adrián Cardil (acardil@tecnosylva.com)

* Both authors contributed equally

Abstract. *In recent years fires of greater magnitude have been documented throughout northwest Europe, and with several climate projections indicating future increases in fire activity in this temperate area, it is imperative to identify the status of fire in this region. This study unravels ~~important~~ unknowns about the state of the fire regime in northwest Europe by characterizing one of the key aspects of fire behavior, the rate of spread (ROS). Using an innovative approach to cluster VIIRS hotspots into fire perimeter isochrones to derive ROS, we identify the effects of land cover and season on fire rate of spread of 102 ~~254~~ landscape fires that occurred between 2012 and 2022~~0~~. Results reveal significant differences between land cover types and there is a clear peak of ROS and burned area in the months of March ~~April~~ and April~~May~~. Median~~Mean~~ ROS within these peak months ~~northwest Europe~~ was approximately 0.09 km/hr ~~0.07~~ during a 12 hour overpass, and 66%~~And However, dDuring the this late spring period, 6667%~~ of the burned area occurs in this spring period.~~, and median fire runs are approximately 0.19070.16 km/hr during a 12 hour overpass.~~ Heightened ROS and burned area values persist in the bordering months of February~~March~~ and May ~~June~~ suggesting that these months may present the extent of the fire season in northwestern Europe. Accurate data on ROS among the represented land cover types as well as periods of peak activity are essential for determining periods of elevated fire risk, the effectiveness of available suppression techniques as well as appropriate mitigation strategies (land and fuel management).*

1. Introduction

Wildfires are among the most common natural disturbances across the globe and play a key role in shaping many ecosystems. In recent years fires have had an emerging impact in areas not traditionally considered fire prone such as the temperate region of northwest Europe. While large and severe fires in these regions were once considered an anomaly, in recent years the occurrence of fires of greater magnitude has been increasing (San-Miguel-Ayanz et al., 2021). In 2020, the Netherlands experienced its potentially largest wildfire in recent history, affecting 710 hectares in the nature reserve of Deurnese Peel (Stoof et al., 2020). In the same vein, the United Kingdom had consecutive

Con formato: Fuente: 10 pto, Cursiva
Con formato: Fuente: 10 pto, Cursiva
Con formato: Fuente: 10 pto, Cursiva
Con formato: Fuente: 10 pto, Cursiva
Con formato: Fuente: 10 pto, Cursiva
Con formato: Fuente: 10 pto, Cursiva
Con formato: Fuente: 10 pto, Cursiva
Con formato: Fuente: 10 pto, Cursiva
Con formato: Fuente: 10 pto, Cursiva
Con formato: Fuente: 10 pto, Cursiva
Con formato: Fuente: 10 pto, Cursiva
Con formato: Fuente: 10 pto, Cursiva

record fire seasons in 2018 and 2019 with burnedburnt areas of 18,032 ha and 29,152 ha, respectively, the largest burned area in the past 10 years (Belcher et al., 2021), most of them affecting peatland areas. Several climate projections suggest increased fire activity in northwestern Europe in the future due to projected drier and warmer weather (Krawchuk et al., 2009; Lung et al., 2013; de Rigo et al., 2017). Moritz et al. ((Moritz et al., (2012)) identified that temperate forests and grasslands are among the most vulnerable biomes at the mid to high latitudes to increases in the probability of wildfires especially in the last three decades of the 21st century (2070–2099). Despite the projected elevated risk, fire behavior within this ecosystem is not well understood. Influential drivers such as vegetation and moisture conditions vary considerably from other parts of Europe such as the Mediterranean where fire and ignition conditions are better researched and understood.

Con formato: Fuente: 10 pto

Fire regimes are defined as long-term patterns of frequency, intensity, and fuel consumption of wildfires in a given area (Keeley et al., 2011). Anticipated changes in local climate are likely to drive alterations in fuels (types, structure, and heterogeneity) as well as conducive fire weather and thus fire occurrence and behavior. Temperate ecosystems, such as those in northwest Europe, which tended to have had limited fire exposure, may become increasingly fire-sensitive and susceptible to increases in fire frequency (McWethy et al., 2013; Kitzberger et al., 2016). Given that fire sensitivity is strongly dependent on interactions between vegetation phenology and fire seasonality, accounting for these factors is imperative when looking at fire behavior (Miller et al., 2019). Timing of phenological events is a major determinant of fuel availability and flammability and within temperate landscapes appears to be driven by changes in temperature (Fares et al., 2017; Chuine and Cour, 1999). The “green up” is likely an important phenological stage when it comes to fire behavior as this is when sap flow begins increasing vegetation moisture. Prior to this green up period, vegetation is drier and may be more susceptible to ignition as fuel moisture is among the most critical parameters affecting fire ignition and propagation (Parsons et al., 2016). *Calluna vulgaris* for example, a shrub commonly found in heathlands, is subject to extremely low fuel moisture levels in early spring as roots still frozen from winter dormancy limit water uptake, posing elevated ignition risks (Davies et al., 2010). Among the different aspects of fire behavior, the rate of spread (ROS) is a key indicator for characterizing fire regimes as it directly contributes to fire size and the overall residence time of the fire (Gill et al., 2008). Forest and fire management depend on accurate knowledge of fire behavior and, particularly, ROS for assessing appropriate fuel treatments (Vaillant et al., 2009). Furthermore, emergency responders such as firefighting operations strongly rely on accurate ROS data to determine their initial and extended attack as well as their fire suppression capabilities. Fires with lower spread rates are generally able to be attacked at the head using hand tools; however, those with higher spread rates will often be more intense and would require special equipment such as dozers and retardant aircraft to be effective (Andrews, 2011). Accurate information on the ROSrate of spread of fires can therefore help increase preparedness of land managers and emergency services across the region.

The relative novelty of fire in northwest Europe means that classifying a fire regime is rather difficult due to the scarcity of data and inconsistencies among record keeping (San-Miguel-Ayanz et al., 2021). European countries vary in their national classifications of fire, the quality of their fire-cause investigations, and the length of time of

national databases (Tedim et al., 2015; Fernandez-Anez et al., 2021). Moreover, national fire databases tend to include data on fire occurrence and cause, but not on fire behavior. Fortunately, remote sensing methods, through the use of satellites, provide spatially and temporally consistent data to permit further analysis of fire behavior, particularly ROS (Sá et al., 2017; Benali et al., 2016). Several studies have proposed methods to extract ROS from satellite imagery using various sensors, such as the Advanced Very High Resolution Radiometer (AVHRR) (Chuvieco and Martin, 1994; Al-Rawi et al., 2001). Several authors have turned to satellite thermal imaging from MODIS (Moderate Resolution Imaging Spectroradiometer) to reconstruct fire progression for larger fires throughout the world (e.g., (Loboda and Csiszar, 2007; Veraverbeke et al., 2014; Jin et al., 2015)). Liu et al. (~~Liu et al., ~~2018) employed the Himawari-8 geostationary satellite to extract the ROS in near real time from grasslands in Australia with promising results. The application of active fire detection products for identifying ROS has the potential to calibrate and validate fire spread models, and several studies have successfully demonstrated methodologies for rapid accurate assessments of ROS in near real time (Sá et al., 2017; Cardil et al., 2019). Many of the aforementioned methodologies and the sensors implemented have been applied in regions where fires tend to be much larger than in temperate Europe, such as in the Mediterranean, California, or Australia (Andela et al., 2019). Our study relies on the Visible Infrared Imaging Radiometer Suite (VIIRS) satellite, which features a higher spatial resolution of 375 m for active fire detection (as opposed to 1 km for MODIS) and may capture more of the smaller fires prevalent in a temperate region.

The objective of this study was to characterize the ROS~~rate of spread~~ of landscape fires within a temperate region facing an increasing risk of wildfires, namely ~~N~~northwestern Europe. We developed a new methodology to derive the rate of spread from hotspots from the VIIRS active fire data product because of its global coverage, near real-time accessible data, and improved spatial and temporal resolution compared to MODIS (Schroeder et al., 2014). Subsequently, we assessed the effects of season and land cover type on rate of spread, as well as differences between countries. A thorough understanding of fires in these emerging regions of northwest Europe will be imperative in developing functional fire management strategies and will serve as a baseline to assess future impacts of climate change.

2. Materials and Methods

2.1 Study area

For the purpose of this study, the boundaries of northwest Europe were defined by the northern Atlantic ~~B~~biogeographical region above 49th parallel based on Sundseth et al., (2009) ~~(above 49th parallel)~~, which ~~and~~ includes many of the traditionally wet countries such as the United Kingdom, Ireland, the Netherlands, Belgium, ~~and~~ Denmark, northern France and northwestern Germany (Fig. 1) ~~(Sundseth et al., 2009)~~. We used the 49th parallel to delineate the boundaries of the study area to focus our analysis in the temperate region of northwest Europe, not traditionally considered fire prone instead of including northern Spain and southern France where fire regimes have

been analyzed in previous research (Moreno and Chuvieco, 2013). The Atlantic b~~B~~iogeographical region is distinguished by an oceanic climate and occupies much of the flat lowlands along the Atlantic coastline. Overall the climate is temperate, marked by its mild winters and cool summers with westerly winds and moderate rainfall throughout the year (Sundseth et al., 2009). The landscape tends to be intensely managed with considerable agricultural areas and expansive industrial and urban regions (Feranec et al., 2010). Nature environments are often isolated and discontinuous due to interwoven urban development spurred by dense populations. The represented vegetation types are diverse and feature heathlands, broadleaf beech forests, meadows, and peat bogs among many others. The ocean drives the climate in this region and as a result it is typically wet and humid for much of the year.

2.2 Visible Infrared Imaging Radiometer Suite (VIIRS) Data

We used data from the Visible Infrared Imaging Radiometer Suite that provides active fire data from the VIIRS sensor aboard the joint NASA/NOAA Suomi National Polar-orbiting Partnership (Suomi NPP) satellite launched in 2011. The VIIRS 375 m active fire product is described in Schroeder et al., (2014) and uses a multi-spectral algorithm to identify fire activity through 5 imagery channels (I-bands), 16 moderate resolution channels (M-bands) and a Day/Night Band (DNB). Specifically, we used the VNP14IMGTDL_NRT near-real time product which has been ~~, a satellite active fire data product~~ widely used in fire modeling applications, in part because of its higher spatial and temporal resolution and accurate ~~compared to other satellites such as MODIS~~response over fires of relatively small areas (Schroeder et al., 2014). ~~NASA's VIIRS was launched aboard the Suomi National Polar-orbiting Partnership (S-NPP) satellite in October, 2011 and has since been providing consistent coverage approximately every 12 hours (Schroeder et al., 2014).~~ Among VIIRS's greatest strengths is the ability to detect at moderate 375 m spatial resolution and provides global coverage approximately every 12 hours (Oliva and Schroeder, 2015); making it an ideal instrument for detecting the smaller fires we anticipated in our study area. VIIRS hotspot data were collected from the NASA Fire Information Resource Management System (FIRMS) portal (https://firms.modaps.eosdis.nasa.gov/) for the period of January 20th, 2012 to June 1st, 2022~~0~~ as no earlier data was available.

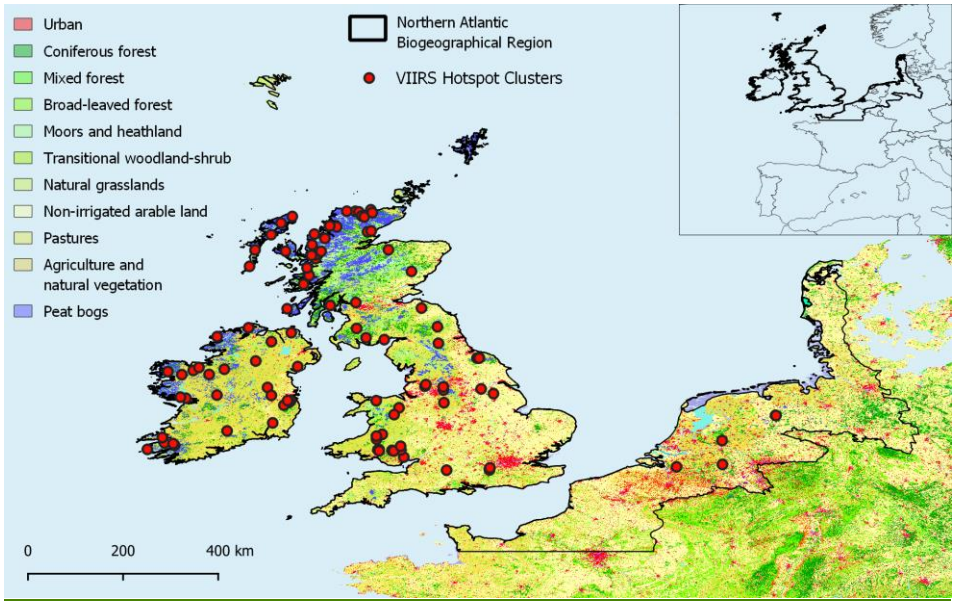

*Figure 1. Study area of northwest Europe, encompassing the United Kingdom, Ireland, the Netherlands, Belgium, Denmark, northern France and northwestern Germany within the northern Atlantic biogeographical region above 49th parallel (Sundseth et al., 2009). Locations of the fire hotspot clusters generated from VIIRS 375 m active fire product (*VNP14IMGTDL_NRT; https://firms.modaps.eosdis.nasa.gov/download/*) derived from 326,935~~344,000~~ hotspot detections from January 2012 through June 2020. Land cover data source:~~map of the study area~~ (*Copernicus Land Monitoring Service's Corine Land Cover Map 2018 (2019a)

Con formato: Fuente: 10 pto, Cursiva

2.2.1 Omission of Non-Landscape Fire Detections

VIIRS sensors detect fires through the identification of mid-infrared radiation emitted from heat sources across the landscape. As these hotspots may also include heat coming from other sources (such as gas flares at industrial sites), it was necessary to screen the VIIRS hotspots to remove thermal anomalies from sources other than landscape fire. As part of this process we overlaid the polygons on the Copernicus Land Monitoring Service's Corine Land Cover Map 2018 ((2019a)) to distinguish landscape fires from other heat sources such as artifacts of heated plumes, or a myriad of other anthropogenic phenomena. VIIRS hotspots identified within a 375m boundary (resolution of VIIRS data) of land cover classified as urban or industrial were excluded from the database.

2.3 Clustering VIIRS data by fire incident based on space and time

~~VIIRS detections are points scattered in time and space.~~ We clustered VIIRS data by fire incident and satellite overpass aiming to develop ROS vectors, characterizing the fire growth. The clustering approach is a three step

process: 1) clustering in space, 2) clustering in time within each previous space cluster, and 3) filtering out clusters with less than 20 VIIRS hotspots, as these are insufficient to derive consistent ROS vectors. The clustering in space was carried out using a grid-growing clustering algorithm. All hotspots are projected into a 5km cell size grid where clusters are defined as groups of interconnected cells in the grid (islands of cells containing hotspots). Cell size and 20 hotspot threshold values were heuristically set. To identify these clusters we loop through the cells in the grid searching for an initial cell containing hotspots but with no assigned ID (not belonging to any cluster). The seed cell is assigned with an ID and then expanded (grown) among neighboring cells containing hotspots using a fast-marching method with 8 degrees of freedom, and assigning all found cells the ID of the initial seed cell. This process is done iteratively until all cells containing at least one hotspot have an ID. The method assures that any hotspot in the cluster has at least one neighboring point within $2\sqrt{2}$ the cell size distance of the grid. ~~The clustering in space was carried out using a grid-based algorithm with the hotspots being reprojected onto a 5 km raster, and neighboring cells containing hotspots were merged to define a cluster area. This process is done by looping through. This technique was chosen because it is much faster than other hierarchical algorithms and does not require a predefined number of expected clusters. This method is intended to assure that any hotspot in a cluster is less than 14 km away from its closest neighboring hotspot in order to properly distinguish different fire incidents. This cutoff distance was determined as the farthest possible distance of two points in neighboring cells with a cell size of 5 km, due to the limitations of the reprojected raster grid resolution. The clustering in time was conducted by ordering the space clusters by time and creating divisions or break points if there was a time difference greater than 48 hours in between consecutive points.~~

Then, the clustering in time was conducted by splitting the initial cluster into subclusters whenever there was a time elapse of 48 hour or more without a hotspot. This threshold value is heuristic and could be slightly modified without significant changes in the final result given that the fire frequently in the study area is usually low. The combined process of clustering by space and time leads to the final group of fire incidents used in the rest of the analysis. ~~The chosen threshold values for the clustering and filtering are heuristic and could be slightly modified without significant changes in the final result. Pre-analysis, these threshold values were adjusted to optimize the balance between the number of fires detected without sacrificing the larger widespread events.~~

Con formato: Fuente: 10 pto

2.4 Generating fire perimeters and ROS vectors

Once the hotspots were classified into individual fires the next step was to generate fire perimeters. At each time step a Delaunay triangulation is constructed using the hotspots from that time step and previous ones. This triangulation method is closely related to Voronoi diagrams and has the important properties of not having intersecting edges, defining triangles with the nearest nodes, and reducing the number of possible interconnecting edges between points. This initial triangulation already contains the lines that will define the final fire perimeter, but to identify them in the triangulation we need to 1) apply an **α**-Shape algorithm, 2) identify the external edges of the mesh, and 3) construct a final geometry out of the individual edges. The **α**-Shape algorithm is applied to the mesh to

remove those triangles whose circumradius (radius of circle circumscribed in a triangle) is greater than 10 km. This process splits the original mesh into independent triangulations if nodes (hotspots) are sufficiently distant from each other, and creates holes inside the mesh if the node density is low. Basically, the value of α determines the maximum distance it is assumed hotspots could define a perimeter edge. In practice, α controls the "porosity" of the final shape since high values lead to a convex hull polygon while lower values increase the concavity of the perimeter. In this analysis the value of α was tested with different values (1, 3, 5 and 10 km), being 10 km the optimal solution to create the fire spread polygons throughout the fire growth. The fire perimeters are now defined by the outer edges of the remaining mesh. These edges can be extracted by noticing that outer edges only belong to one triangle in the mesh while internal edges are shared between two triangles. Extracted edges are then ordered to form valid geometrical polylines and then aggregated together to form the final polygons representing the fire perimeters.

Notice that in this process the perimeter exactly connects the input hotspots without considering the actual VIIRS spatial resolution. This could be easily fixed by applying an external buffer to the perimeter equal to half the resolution distance of VIIRS (around 375 m). In any case, it is important to notice that this does not affect the ROS calculation since the same procedure is used at each time step, and therefore the distance between consecutive perimeters is not affected.

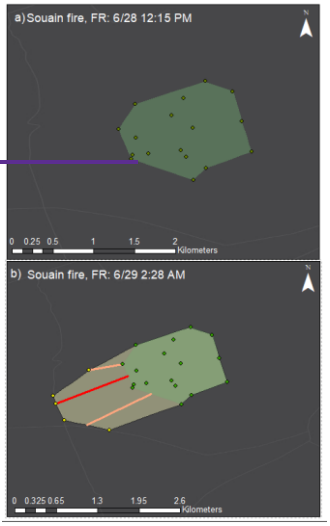
a) Souain fire, FR: 6/28 12:15 PM
0 0.25 0.5 1 1.5 2
Kilometers
b) Souain fire, FR: 6/29 2:28 AM
0 0.325 0.65 1.3 1.95 2.6
Kilometers

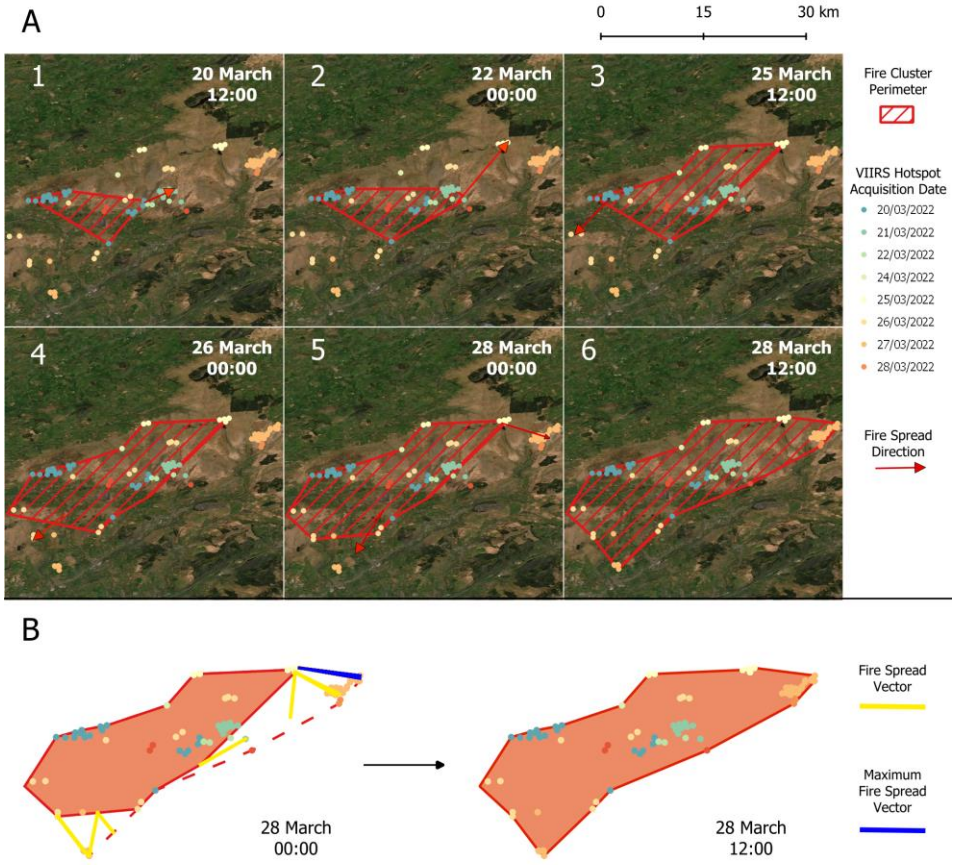

Figure 2. Multipolygons and ROS spread vectors for the Mynydd Mawr fire in Wales (March 20, 2022), representing the methodology used to delineate fire perimeters and Rate of Spread (ROS) vectors. A) Scheme of the fire growth in several time steps throughout the fire duration delineated using the VIIRS hotspots (VIIRS 375 m active fire product at each satellite overpass (VNP14IMGTDL_NRT; https://firms.modaps.eosdis.nasa.gov/download/). Red arrows represent the main fire spread direction schematically.

B) Real ROS vectors (yellow lines) and perimeters generated (orange polygons) in two selected satellite overpasses. For each time step, the maximum ROS vector is selected for further analyses (blue lines), representing the ROS in the head of the fire.

With the fire progression multipolygons developed, the rate of spread vectors could be calculated. For each vertex of the polygon at time t+1 the closest vertex of the parent polygon at time t was identified. Taking into consideration the distance and time between both points, we calculated the ROS of each spread vector (Fig. 2). To increase the accuracy of the spread vectors, the number of vertices at each polygon and time step was increased by adding one extra node between neighboring points

~~**2.5 Omission of Non-Landscape Fire DetectionsFalse Detections**~~

~~VIIRS sensors detect fires through the identification of mid-infrared radiation emitted from heat sources across the landscape. As these hotspots may also include heat coming from other sources (such as gas flares at industrial sites), it was necessary to screen the derived ROS clusters to remove thermal anomalies from sources other than landscape firefor false detections. As part of this process we overlaid the polygons on the Copernicus Land Monitoring Service's Corine Land Cover Map 2018 ((2019a)) to distinguish landscape fires from other heat sources such as active volcanoes, artifacts of heated plumes, or a myriad of other anthropogenic phenomena. Polygons identified within a 1 km boundary of land cover classified as urban or industrial were excluded from the database.~~

2.5~~6~~ ROS Classification and Analytical Methods

Each individual fire contained many vectors for ROS at each vertex for each timestep representing the fire progression in every direction (see an example in Fig. 2). In order to identify the widely utilized head of the fire we grouped vectors by fire and timestep and filtered out the maximum ROS value for each fire and time step. As each timestep also featured data on land cover, country of origin, and the month of incidence it became possible to draw comparisons between variables. ~~There were some issues within the clustering process that permitted fires with greater distances to be classified as an individual event, which led to erroneous extreme ROS rates. To account for this, all extreme spread vectors were checked manually for mistaken groupings and if identified as such excluded from the dataset. Remaining VIIRS ROS vectors were then grouped by their associated country, land cover, and month to determine the effects of season and land cover on fire spread.~~ We used ~~using~~ a one-way ANOVA (Girden, 1992) and Tukey post-hoc statistical analysis to identify significant associations between ROS and land cover types. Also, we evaluated relationships between ROS ~~vectors magnitude, as max values,~~ and fi~~nal~~ size~~burned area generated in every single fire~~ through a linear model approach, transforming the variables as needed to meet the model requirements of homoscedasticity and linearity~~model fitting~~.

3. Results

3.1 Distribution of fire detections and classification of fire events

The 326,935~~344,048~~ individual fire detections identified in our study area were filtered into 29,215 detections on wildland areas and grouped into ~~2,543 clusters, of which~~ 1022~~54 were verified to be~~ "real" landscape fires. ~~and not~~

~~as an artifact of permanent hotspots or thermal plumes~~ Within these fires, we identified 327 ~~maximal~~ ROS vectors which represented the ROS in the head of the fires for each satellite overpass throughout the fire growth and~~, which~~ were used for further statistical analysis. The greatest number of fires was registered in the British Isles while detections were really scarce in continental Europe within the study area. In fact, ~~T~~there were no fires identified ~~registered~~ for the study period in Belgium~~, and~~ Denmark and France. The final output for each fire included~~:~~ timing polygons and burned~~burnt~~ area for each time step. For spread vectors, land cover and ~~maximum~~ ROS vectors by time step throughout the fire duration were~~as~~ identified.

3.2 Burned~~Burnt~~ Area

Peak burn area across the study region occurred in the months of March~~April~~ (40~~43~~%) and April~~May~~ (26~~24~~%) when 66~~67~~% of the total burned~~burnt~~ area was observed (Fig. 3a). In April ~~March~~ there was a greater percentage of fires (41~~23~~%) compared to March~~May~~ (20~~13~~%~~) although they contributed to a smaller percentage of overall burned~~burnt area~~, indicating that while fires in April~~March~~, may be more frequent they are also smaller. ~~There was a second smaller peak of increased burned~~burnt area in July consisting of fires from 2018, which amounted to nearly 14% of total burned area~~ Therefore, ~~T~~there~~'s~~ is ~~a~~ clearly defined peak fire season: from March and April. Beyond this fire season peak, ~~F~~fire activity starts increasing in February and~~. Also,~~ decreasing~~to decline starts~~ in May and more especially in the summer~~from then on is scarce~~ (Fig. 3a). In terms of size, 54% of fires are smaller than 10 km2. ~~On the other hand, f~~Fires exceeding 40 km2 were 13% of the generated clusters (Fig. 3b). Mid-sized fires (from 10 to 40 km2) comprised 33% of total wildfires.~~In terms of fire size, nearly 80% of the burned area was caused by wildfires between 1-10 km^2 (Fig. 3b). These mid-sized fires comprised half of the total fires detected. Fires exceeding 10 km^2 made up approximately 13% of the total burned~~burnt area but only 2% of total wildfires. On the other hand, fires less than 0.01 km^2 were rarely detected with our satellite-based analysis, comprising approximately 0.002% of the total burned area and 1% the total number of fires. Fires between 0.01–0.1 km^2 were also seldom observed with 0.3% of the burned~~burnt area set by 10.2% of total fires.

Con formato: Fuente: 10 pto

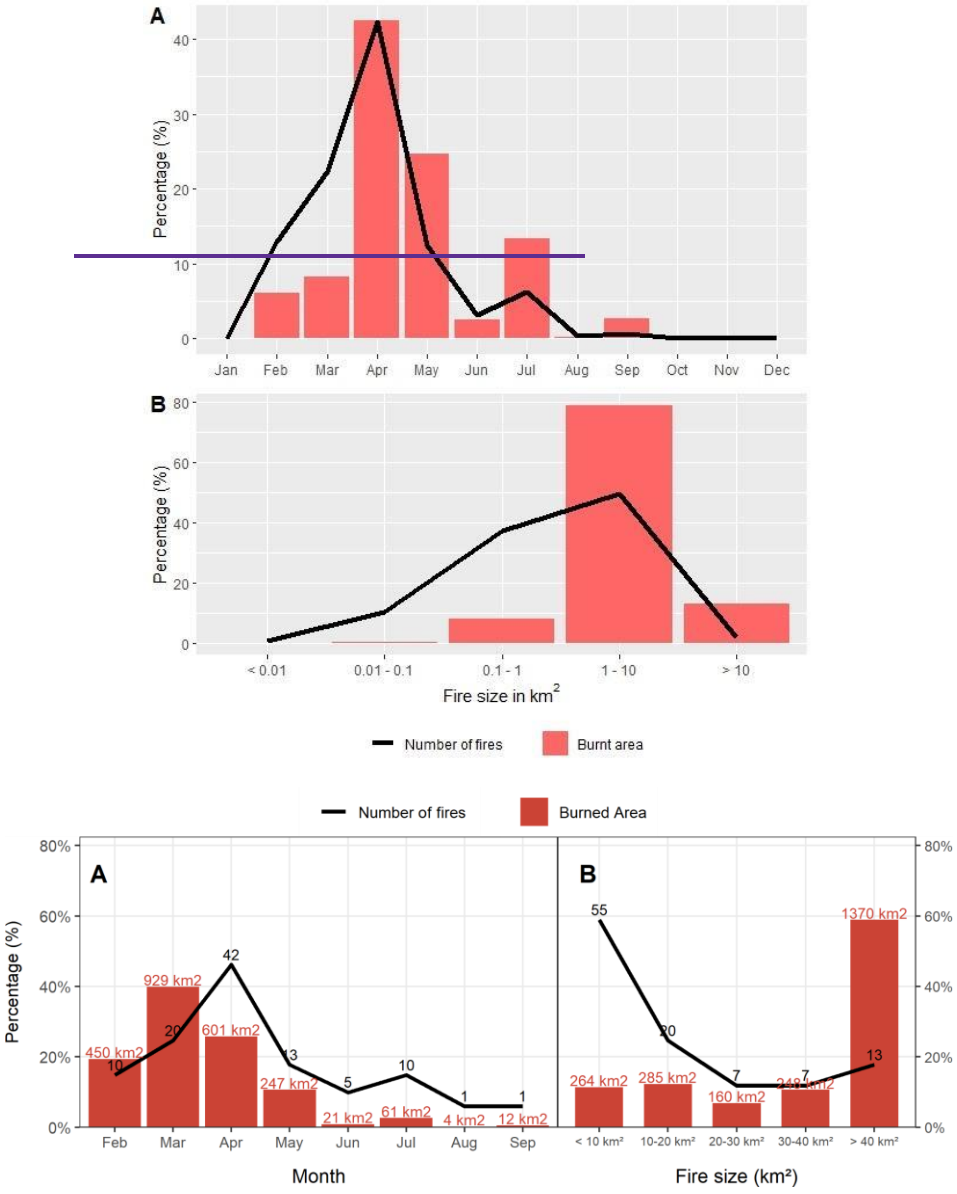

Figure 3: Burned~~Burnt~~ area percentages for ~~n~~Northwest Europe calculated a) monthly and b) according to size distribution at the time the fire ended. Notice that this burned~~burnt~~ area may not be the same as that detected by other remotely sensed burned~~burnt~~ area products, or delineated in the GIS systems maintained by fire managers due

Con formato: Centrado

to the spatial resolution limitations of the active fire product used in this work (VNP14IMGTDL_NRT; https://firms.modaps.eosdis.nasa.gov/download/).

3.3 Effect of Season on Rate of Spread

Trends for the northwestern European area indicated that the months of February, ~~April,~~ March and April ~~May~~ witness the most active fire activity (Fig. 4a). It was during this period that the median ROS was the greatest (0.13~~15~~ km/hr, 0.09 and ~~0.12~~0.09 km/hr, respectively), and this was reflected in the greater burned area, exceeding 1,981~~500~~ km^2 ~~for both months~~ (Fig. ~~4a~~3a). ROS from ~~in~~ February to April ~~March also~~ registered ~~quite~~the ~~highest~~highly ROS values, concurring ~~indicating~~ the~~with a~~ peak values of the year. ~~median of 0.130.11 km/hr~~. The remaining months of June, July, August, September and January ~~February, June, July, and September~~ featured a median ROS lower than 0.05 ~~of 0.068~~ km/hr, and this also reflects the variation in burned area: a reduced value of around 98 km2 in these months (Fig. 4a). ~~~~Mean ROS within northwest Europe was approximately 0.07 ~~0.19~~ km/hr for the entire study period, with half of our ROS observations falling within the 0.04 ~~0.04~~ km/hr to 0.14 ~~0.28~~ km/hr range (Fig. 4a). The data revealed that for the fires considered, 12-hour spread rates rarely exceed 0.34 ~~0.5~~ km/hr. ~~Fires at the tail ends of this timeframe in August and September registered among the lowest spread rates comparatively, and this is reflected in the reduced accumulated burn area of around 100 km^2 in these two months (Fig. 4a).~~

Zooming into the country level, across northwest Europe landscape fires were detected from January ~~February~~ to September, predominantly in February, March and April~~April and May~~ (Fig. 4b). Peak ROS for England, Ireland, Scotland and Wales~~England, Ireland, Scotland, and Northern Ireland~~ was found in late winter to ~~spring and~~ spring ~~earlier summer~~ months. Germany and The Netherlands ~~and northern France~~ only detected fires in a couple ~~single~~ months ~~month but they both tend to match the trend~~. Fires observed for Germany, The Netherlands and Northern Ireland~~both Wales and Germany~~ appear to deviate from this pattern. Germany reached its peak ROS in September, The Netherlands in April and Northern Ireland in May. ~~Nevertheless, these 3 regions have few fires: 2, 2 and 4, respectively.~~

~~Germany reached its peak ROS in February and further fires were not detected by VIIRS until the end of summer months in July and September. Furthermore, the ROS captured in February was the highest recorded at 1.4 km/hr. Wales, like Germany, reached its highest ROS in February but the values were not all that different in the following months.~~

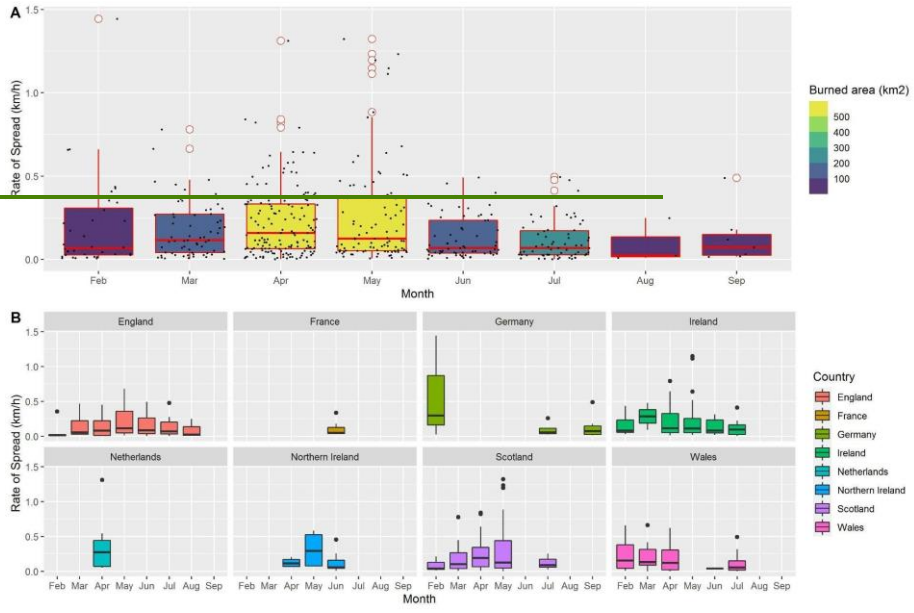
A
Rate of Spread (km/h)
1.5
1.0
0.5
0.0
Feb
Mar
Apr
May
Jun
Jul
Aug
Sep
Month
Burned area (km2)
500
400
300
200
100
B
England
France
Germany
Ireland
Netherlands
Northern Ireland
Scotland
Wales
Country

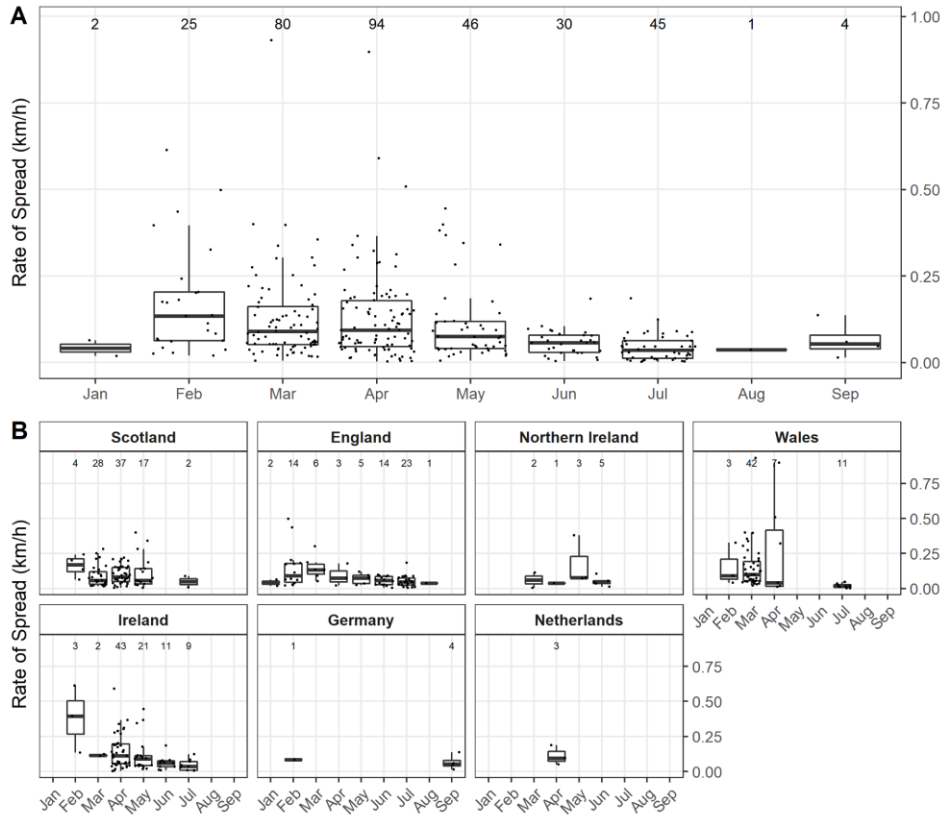

Figure 4: Rate of spread for northwest Europe from 2012–2020 calculated monthly A) for the northwest European area (northern Atlantic biogeographical region) and B) per country. Points represent sample size and it is also indicated as numbers on top of each boxplot. Fires were not detected for months not represented in the figure.

3.4 Land Cover Effects on Rate of Spread

The number of ROS vectors differed across cover types, being the peat bogs and moors and heathlands the most representative cover types of wildfire activity. The ~~Rate of spread clearly differed across cover types (Fig. 5). S~~statistical analyses revealed significant effects of land cover on ROS (p=0.03; Fig. 5). Fire spread through coniferous forests had the highest ROS ~~rate~~ with a mean of 0.19 km/h whereas fires spreading on ~~. T~~ transitional woodland-shrubs had ~~was~~ the s~~lowest~~ average ROS~~cover~~ with a value of 0.04 km/h ~~mean~~. The ~~D~~differences in ROS between these two types of land cover w~~as~~ere significant (~~, as was shown in the~~ in the post-hoc analysis (p=0.01)). Natural grasslands, Peat bogs, Moors and heathland and Pastures~~Other~~ cover types had average ranging

values between 0.08 and 0.14 km/h ~~them therefore~~ and no statistical differences were found among these cover types (Fig. 5). ~~there were no other significant differences.~~

~~Statistical analyses did not reveal statistically significant effects of land cover on ROS (p=0.13). Differences between land cover types were small, with a mean difference of approximately 0.13 km/hr between the highest and lowest land covers (Fig. 5) Peat bog vegetation showed the greatest mean ROS at approximately 0.21 km/hr. On the other end of the spectrum were the mixed forests with a mean spread rate of approximately 0.077 km/hr and pastures at 0.1 km/hr. Coniferous forest, transitional woodland-shrub, and natural grasslands all exhibited similar mean spread rates of approximately 0.12 km/hr. Moors and heathlands, broad-leaved forest, and land principally occupied by agriculture, with significant areas of natural vegetation, all featured mean ROS on the higher end of the scale ranging from 0.15 to 0.175 km/hr (Fig. 5).~~

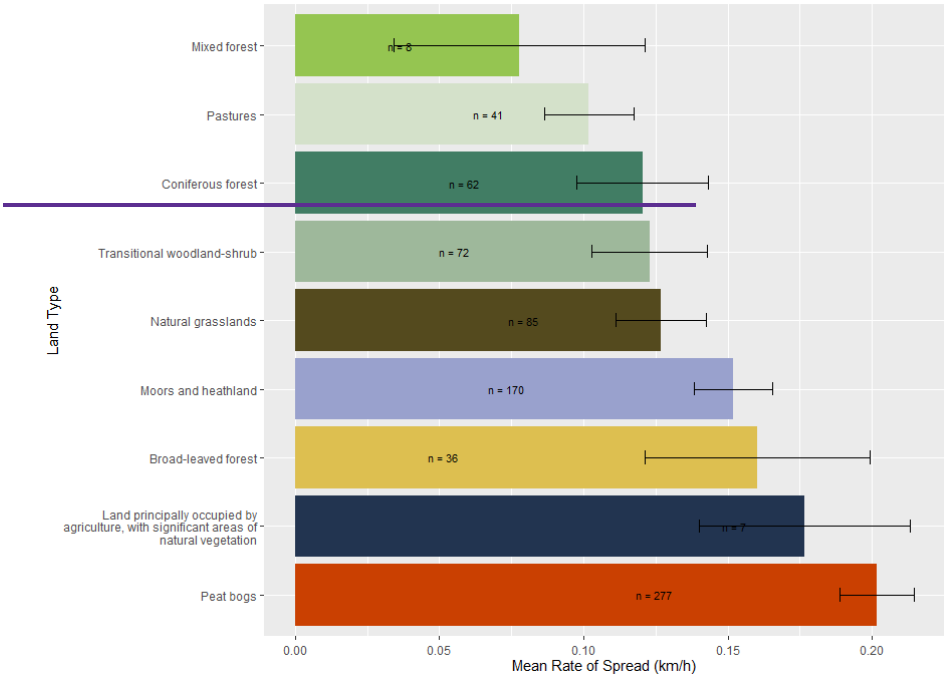
Mixed forest
Pastures
Coniferous forest
Transitional woodland-shrub
Natural grasslands
Moors and heathland
Broad-leaved forest
Land principally occupied by agriculture, with significant areas of natural vegetation
Peat bogs
n = 8
n = 41
n = 62
n = 72
n = 85
n = 170
n = 36
n = 7
n = 277
Land Type
0.00
0.05
0.10
0.15
0.20
Mean Rate of Spread (km/h)

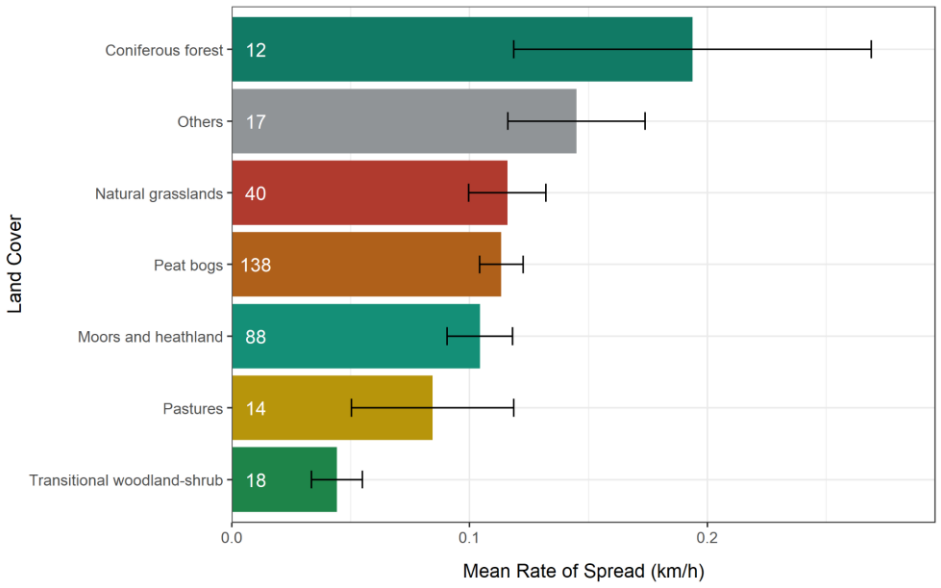

Figure 5: Mean Rate of Spread and standard error across various represented land cover types in northwest Europe. The category "others" includes other land cover types with low representation (less than 10 maximum spread vectors by category). The number of ROS vectors for each land cover type is shown in the chart. ~~Number of observations pointed in numbers for each type.~~

3.4 Relationships between ROS ~~vectors magnitude~~ and ~~final~~ burned area

*The l~~L~~*inear regression model found~~outputs a~~ significant the relationship between ROS and final burned area ~~model of log(Burned Area) ~ log(Maximum ROS) with the independent variable as a significant predictor~~ (Fig. 6). The model yields a R^2 value of 0.4 and~~.~~ Subsequent analysis confirmed that residuals are normally distributed and with homoscedasticity. The slope ~~C~~coefficient of the model~~for the predictor~~ is positive, indicating that high~~er~~ values of ROS~~maximum spread vectors~~ likely end up in a large burned area.

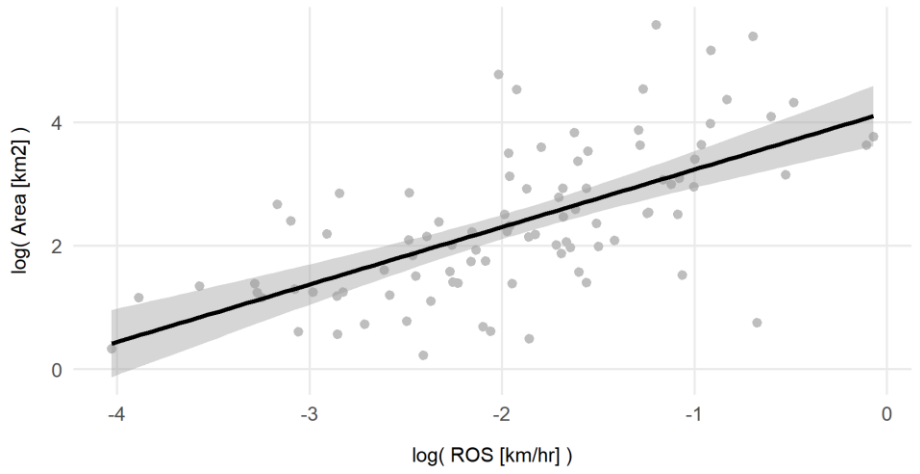

Figure 6 : Linear regression model for log-transformed variables (Rate of Spread, ROS; and burned area) indicating a positive relationship between ~~maximum rate of spread (ROS) vectors~~ and final burned area for each fire.

4. Discussion

4.1 Burned Area & Peak Activity

The analysis of the intra-annual burned area is essential for determining periods of peak fire risk and impacts. Our results clearly indicate a major peak in burned~~burnt~~ area in late winter and spring (March and April ~~April and May~~) ~~but also a second minor peak in mid summer (July)~~ (Fig. 3a). ~~This secondary peak in July was composed entirely from fires in the UK during 2018, a summer in which there was extensive drought and heatwave across northern Europe (Fu et al., 2020)~~. Summer fires are unusual as they occur following the spring green up period when the vegetation moisture is typically high, hence large fires in temperate summer tend to require considerable arid conditions or drought. It is acknowledged that our data record of nine years occurs within longer-term fire activity and climate cycles that may influence the trends observed; however, these findings are in agreement with research reporting fire seasonality using longer-term data sources (e.g., Belcher et al., 2021). Regarding fire size, our analysis identified that most of the burned area was contributed by fires larger than 40 km^2 with equal ~~slight~~ contributions from fires in the 30-40~~0.1 1~~ km^2 , 20-30 km2, 10-20 km2 and 10 <~~>10~~ km^2 scales. This indicates that ~~mid to~~ large size fires are responsible for most of the total burned area rather than smaller fires. The lack of fires smaller than 10 km^2 can likely be explained by the fact that the VIIRS satellite was unable to capture fires of this magnitude due to limitations of the temporal and spatial resolution (Schroeder et al., 2014) and may also be because of the minimum

Con formato: Fuente: 10 pto, Color de fuente: Negro

Con formato: Fuente: 10 pto

threshold of 20 hotspot points to derive ROS vectors. Smaller fires are much more ubiquitous than larger fires as fire size distribution commonly follows the power-law function (Cui and Perera, 2008; Hantson et al., 2015). While it is likely that these smaller fires are more frequent than indicated, fires of this scale are less likely to be significant contributors to overall burned area (San-Miguel-Ayanz et al., 2021). Moving forward, it is important to consider that the fires included in this study are of mid to large size rather than smaller fires especially when it comes to estimating the ROS as smaller fires are likely to reduce the mean ROS, ~~,~~ despite the fact that some small fires may have experienced high ROS over short time periods.

Of the 102 ~~254~~ fires considered in this study, It is unlikely that any were prescribed burns as most of the fires accounted for were outside the main prescribed burn window of October to March. Moreover, all of our fires burned overnight and prescribed burn codes in the study region do not permit burning overnight ((Heather and grass burning: rules and applying for a license~~licence~~, 2021; Guidance - The Muirburn Code, 2021; Department of Agriculture, Food and the Marine, 2021)). Furthermore, our clustering algorithm required a minimum of 20 hotspots to be identified as a potential fire, which is unlikely for a prescribed burn.

4.2 Spread Rates & Peak Activity

Spread rates were calculated for various countries throughout the year and for various land covers in a region where fire behavior data tend to be scarce with a limited history of records. The seasonal rate of spread analysis indicates peak burn area and ROS in the months of March and April ~~and ROS in the months of March and April~~ (Fig. 3 & 4). The bordering month~~s~~ of February and May ~~also featured heightened rate of spread and burned~~burnt area values suggesting that February and May might ~~March through June may~~ present the extent of the peak fire season in northwest Europe. The fire season is likely longer than indicated within our study but due to sensor limitations (spatio-temporal resolution of data (Schroeder et al., 2014)) we are unable to capture and account for the smaller fires and can only ascertain periods of peak activity of the larger fires. While studies on fire regimes within this region are scarce, the timing and duration of the peak of fire season outlined in our study is in agreement with the fire season set out in various literature. De Jong et al. (de Jong et al., 2016) concluded that a majority of wildfire activity in the United Kingdom occurs from March to May (59% of events and 95% of the burn area). Likewise, the Irish Department of Agriculture, Food and Marine (DAFM) distinguishes the period of heightened fire risk from the months of March to June (Fire Management, 2021), and within the Netherlands, peak fire activity is typically in the spring and early summer (April to June) (San-Miguel-Ayanz et al., 2019)

The March ~~–~~April~~March–June~~ spring fire season identified in northwest Europe is a clear contrast to the Mediterranean fire season, which features a minor peak in spring but a stronger peak towards the months of July–September, at the later end of summer (Pausas and Paula, 2012; Le Houérou, 1973). The Mediterranean fire peak culminates in summer as the fuel moisture is lowest during this period within this climate (Chéret and Denux, 2007). However, this likely differs in northwest Europe where the temperate climate is typically wetter and more humid in

summer, and the period of lowest fuel moisture tends to fall before the phenological green up period in late spring. Davies et al. (Davies et al., 2010) reviewed temporal variations in moisture for *Calluna vulgaris* across Scotland and identified consistently low live fuel moisture contents in spring and consistently high moisture contents in summer which were largely attributed to the flush of young green summer growth. Davies et al. 2010 also noted that vegetation moisture might be more sensitive to changes in weather conditions than seasonal trends considering the rapidity of changes therefore combinations of low nighttime temperatures, frozen ground, and relatively warm sunny days in the early spring may lead to elevated fire hazards. Significant correlations have been widely observed between wildfires and the phenological stages of vegetation across southern Europe (Moreira et al., 2009; Angelis et al., 2012), it is possible that local phenology plays a role in the differences in peak fire activity in northwest Europe. The phenological cycle alters key characteristics of fuels including biomass, spatial distribution, moisture content, and chemical composition, which are key determinants for fire behavior (Fares et al., 2017). Further research is needed to identify linkages between vegetative phenology, meteorological conditions, and fire occurrence in this region.

4.3 Effect of Land Cover Type

Our study did find a Surprisingly, our study did not yield any statistically significant effect of land cover on ROS. Land cover has been shown to be among the main drivers of fire intensity and ROS through its influence on plant biomass, vegetation structure, and moisture content (Moreira et al., 2009). In a similar study, Loboda and Csiszar (2007) also reconstructed fire spread across Eurasia using MODIS and derived ROS and found significant effects of ecoregions. However, we recognize limitations in terms of satellite fire detection andecoregions are of greater spatial scale and resolution of do not account for the finer distribution of different vegetation type maps. ThusIn this sense, Ffuture studies could benefit from the use of high-resolution fuel maps, which were not yet available at this time, rather than coarse land cover when investigating links to ROS. Land cover may not be able to sufficiently encompass the complexity of fuel types present and, therefore, enhanced fuel type maps may allow further exploration of these relationships. . Perhaps a reason for the lack of significant differences between land types and ROS is that they may often contain similar vegetation.

The ROS analysis among various land cover types yielded coniferous forests as the fastest spreaders. It was expected that coniferous-type vegetation had higher values of ROSspread, as it is documented that, in mediterranean regions, this cover type has more fire-selectivity in heterogeneous landscapes, being qualified as one of the most fire-prone among vegetation types (Barros and Pereira 2014). In our study area, most coniferous forests were distributed in the British Iisles and our proposed methodology identified several fire clusters associated with severe and complex fires such as Ceredigion Fire (~43 km2 in 8 days March, 2022), Galway Fire (~59 km2 in 4 days. May, 2019), Sliabh Beagh Fire (~38 km2 in 2 days May, 2017), in which there was important coniferous vegetation areas that were burned area. Despite that there were a small number of fires spreading on few observations regarding coniferous forests, previously exposed data and statistical difference in this type of cover denotes importance for further studies regarding coniferous

or woodland-type covers in Northern Europe Fires. Moors-heathland and Peat bogs had the highest number of spread vectors in this study though represented moderate ROSaverage spread rates compared to coniferous forests among cover types. These two cover types accounted for 1% of wildfires in the UK and were responsible for between 4 and 82% of the total burned area and included some of the more high profile fires in recent years, such as the ~1,000 ha Saddleworth Moor fire (2018) and the ~16.000 ha Knockando fire (2019), as reported by The UK Forestry Commission (2019). Gazzard et al., (2016) performed an analysis of wildfire incidents from the Incident Recording System data in the UK and identified that these moorland and bog fires account for 40% of the area burned in the region due to horizontal continuity of fuel, topography, and difficulty of suppression, which permits fires to spread. Consequently, this work points out how different land covers can reach similar values of burned area in the end, but at completely different ROSrates of spread. This has important implications for fire management, depending on the coverage present in the landscape.

The ROS analysis among various land cover types yielded coniferous forests as the fastest spreaders and the coniferous and mixed forests as among the slowest (Fig. 5).Among peatlands, fire spread is dominated by flaming combustion of surface fuels like grasses and shrubs (Santoso et al., 2019). The ROS being observed on this land cover are due to the surface fires spreading via the vegetation on the top layer and can include a number of mosses, herbaceous plants such as *Molinia*, woody plants, and dwarf shrubs (CLC). The aforementioned vegetation is not unique to peatlands and can also be found within the heathland and moorland land covers. The Forestry Commission ((2019b)) reported that while mountain, heath, and bogs only accounted for 1% of wildfires in the UK these fires were responsible for between 4 and 82% of the total burn area and include some of the more high profile fires in recent years, such as the ~1,000 ha Saddleworth Moor fire (2018) and the ~16,000 ha Knockando fire (2019). Gazzard et al., (2016) performed an analysis of wildfire incidents from the Incident Recording System data in the UK and identified that these mountain, moorland, and bog fires account for 40% of the area burned in the region due to horizontal continuity of fuel, topography, and difficulty of suppression, which permits fires to spread. Open habitats, or landscapes not enclosed by trees, such as heathlands, typically permit greater surface wind speeds in the absence of obstacles and allow for uninterrupted fire spread (Linn and Cunningham, 2005). Within the Corine Land Cover classification map, most of the fire incidents on peat bogs within our study are located on more mountainous terrain in the Scottish highlands, which contain Flow Country, home to the largest peat bog in Europe, and the west coast of Ireland. There may be several potential reasons for the higher ROS within these areas, including possible synergies between topography and strong Atlantic winds, remoteness contributing to difficulty in accessibility or water availability limiting suppression, or greater horizontal fuel continuity from peat to surface vegetation and further research is required to explore these linkages.

Zooming in on the land cover type where rate of spread was slowest, mixed and coniferous forests exhibited among the slowest spread rates observed at 0.077 and 0.12 km/hr, respectively (Fig. 5). Between 2009–2017, woodland and forest fires accounted for less than 5% of the total burned area in the UK (Forestry Commission England, 2019). A plausible explanation for the slow ROS in these forests is that fires in these systems are wind-limited due to a more closed canopy; therefore, they may tend to be slower moving (Cochrane, 2003).

Overall, the ROS values were low to moderate. The fastest spreading fuel type, coniferouspeat bog vegetation, only recorded a mean ROS of approximately 0.190.22 km/hr, which is not considered to be a fast moving fire. The reason for such low values may lie within the methodology implemented, which produced average spread rates. The ROS vectors were derived from the VIIRS satellite which has an overpass time of 12 hours. Developing the ROS vector over such a long time frame is likely to underestimate the actual ROS: it is unlikely that the fire progressed at a constant rate over the course of the timestep, especially as we are averaging the ROS over periods of night and day. Therefore there is a degree of variation that should be taken when relying on these estimations from VIIRS. This may also be the reason why there appears to be less variation among the different land cover types.

3.4 Relationships between ROS vectors magnitude and final burned area

It was expected to find a relationship between ROSfire propagation and final burned area although there are many factors influencing the fire growthimplied within this phenomenon, includingboth environmental variablesdynamics and fire suppression actions. We found a positive significant relationship The result of the fitting process found a good significant model that meets all the assumptions, indicating that there is a statistical positive relationship between ROSfire rate of spread and the finaland final burned area. Peatland fires, land cover with the highest number of observation in this study, account for one of the highest burned areasarea in the world (Rein and Huang, 2021), burning surface vegetation and underground smoldering of peat soils with probably the slowest ROS among land cover types (Huang and Rein, 2017) An alternative escenario of a negative relationship, with high burned area and slow propagation fires would have been expected for peatlands, one of the main cover types in this work, because these type of fires are characterized for having one of the highest burned area in the world (Rein and Huang, 2021) and the slowest rate of spread among fire types (Huang and Rein, 2017). The VIIRS satellite probably did not capture smoldering fires and only surface fires which would represent the fires with the highest ROS values for this cover type. On the other hand, high values of spread rates correlated with lower burned area values would have indicated strong suppression efforts. Hence, our findings pointed out the existence of a dynamic in which fast-spreading fires ignitions frequently end up in large burned areas consumed by fire in northwesternnNorthernwestern Europe.

4.4 Implications for Fire Management

Accurate data on ROS among the represented land cover types as well as periods of peak activity are essential for determining periods of elevated fire risk, the effectiveness of available suppression techniques as well as appropriate mitigation strategies (land and fuel management). While this knowledge is abundantly available for regions that are familiar with wildfires, emerging fire prone regions often lack research in part due to limited records and past fire exposure. northwest European forest and fire managers may use these results to inform people that they should be wary or prepared for incidents of wildfire in the months of MarchApril and AprilMay or even in late springlater in

~~summer~~ in years of severe drought (Fig. 3 & 4). These managers and fire suppression experts may also consider that the values for ROS are likely to be underestimated due to the methods implemented, particularly the averaging of ROS over 12 hour periods.

Knowledge of the underlying conditions permitting fire spread will be essential for determining appropriate suppression methods. Furthermore there is a need to account for the prevalent smaller fires that are not captured by VIIRS. Even fires of smaller magnitude have the potential for widespread impact due to a higher urban density throughout northwest Europe. Estimates for ROS of these smaller fires may require a more ground-based approach until there is development towards a monitoring system of satellite sensors with higher spatial and temporal resolution such as that of the Canadian WildFireSat suitable for real time emergency management (Johnston et al., 2020). Higher resolution information pertaining to fuels will be necessary for identifying at risk vegetation types as well as for capturing fuel heterogeneity permitting fire spread. If increases in fire activity within this northwest European region are to be expected, it will be crucial to not only prepare for the fires experienced now, but ones of more adverse behavior. Steps towards characterizing the current and future fire behavior in this region should be further addressed to ensure future risks can be properly approached and mitigated.

5. Conclusions

The findings obtained in this study provide among the first estimations of wildfire ROS~~rate of spread~~ for northwest Europe and present a novel methodology towards the characterization of fire behavior in this newly fire prone region through the use of satellite hotspot detection. This technique identified 102 fires and has proven to be a useful alternative in the absence of infield measurements and years of data collection. This allowed us to characterize the ROS on different land cover types in northwest Europe and identify ~~and define~~ peak months of fire activity~~damage caused by forest fires and, therefore~~, providing key ~~giving indications~~information for efficient fire management ~~of resources destined for prevention and suppression~~. It was also possible to establish a relationship between the ROS~~rate of spread of a fire~~ and the final area burned in this area of Europe, characterized by~~which has~~ different environmental conditions compared to ~~commonly~~ studies developed in southern Europe~~d regions. Within this, coniferous forests could be identified as a type of cover that has a higher spread rate than the others, giving out prior information for a landscape-based planification for wildfire management.~~

~~Regarding the seasonality of fires within northwest Europe, the months of March and April were identified as periods of peak fire activity in terms of heightened ROS and burned area. During this peak, 66% of the burned area occurs. Median fire runs are approximately 0.07 km/hr during a 12 hour overpass for the entire study area. There was a significant effect of land cover on ROS, this was observed between two cover types: Coniferous forests and Transitional woodland-shrub. Among the represented land covers, coniferous vegetation had the highest mean ROS of 0.19 km/hr, while transitional woodland-shrub vegetation had the lowest of 0.04 km/hr.~~ Steps towards characterizing the fire behavior in this region should be further addressed to ensure future risks can be properly approached and mitigated. Future analyses to characterize fire behavior and fire regime in northwest Europe should consider the fire frequency, duration, as well as the meteorological conditions contributing to ignitions.

Data availability. The data collected and produced is available on the Zenodo platform. The DOI and link of access is https://doi.org/10.5281/zenodo.6330201

Author Contributions. M.T. and A.C. conceived the idea; S.M. developed the algorithm and ran the analyses; M.T., T.Q. and A.C. ran subsequent analyses and interpretation; M.T. led the writing of the manuscript; A.C. led the review of the manuscript after reviewers' comments and suggestions. All authors contributed critically to writing and editing the drafts and gave the final approval for publication.

Competing Interests. The contact author has declared that neither they nor their co-authors have any competing interests.

Acknowledgements. This project has received funding from the European Union's Horizon 2020 research and innovation programme under the Marie Skłodowska-Curie grant agreement No 860787 (PyroLife Innovative Training Network https://pyrolife.lessonsonfire.eu/), a project in which a new generation of experts is trained in integrated fire management.

References:

Al-Rawi, K. R., Casanova, J. L., and Romo, A.: IFEMS: a new approach for monitoring wildfire evolution with NOAA-AVHRR imagery, Int. J. Remote Sens., 22, 2033–2042, 2001.

Andela, N., Morton, D. C., Giglio, L., Paugam, R., Chen, Y., Hantson, S., Van Der Werf, G. R., and Randerson, J. T.: The Global Fire Atlas of individual fire size, duration, speed and direction, Earth Syst. Sci. Data, 11, 529–552, 2019.

Andrews, P. L.: How to generate and interpret fire characteristics charts for surface and crown fire behavior, US Department of Agriculture, Forest Service, Rocky Mountain Research Station, 2011.

Angelis, A., Bajocco, S., and Ricotta, C.: Phenological variability drives the distribution of wildfires in Sardinia, Landsc. Ecol., 27, 1535–1545, https://doi.org/10.1007/s10980-012-9808-2, 2012.

Barros, A. and Pereira, J.: Wildfire Selectivity for Land Cover Type: Does Size Matter?, PLoS ONE 9(1): e84760. https://doi.org/10.1371/journal.pone.0084760. 2014

Belcher, C. M., Brown, I., Clay, G. D., Doerr, S. H., Elliott, A., Gazzard, R., Kettridge, N., Morison, J., Perry, M., and Smith, T. E. L.: UK Wildfires and their Climate Challenges, E Third UK Clim. Change Risk Assess. CCRA3, 79, 2021.

Benali, A., Russo, A., Sá, A. C. L., Pinto, R. M. S., Price, O., Koutsias, N., and Pereira, J. M. C.:

Determining Fire Dates and Locating Ignition Points With Satellite Data, Remote Sens., 8, 326, https://doi.org/10.3390/rs8040326, 2016.

Cardil, A., Monedero, S., Ramírez, J., and Silva, C. A.: Assessing and reinitializing wildland fire simulations through satellite active fire data, J. Environ. Manage., 231, 996–1003, https://doi.org/10.1016/j.jenvman.2018.10.115, 2019.

Chéret, V. and Denux, J. P.: Mapping wildfire danger at regional scale with an index model integrating coarse spatial resolution remote sensing data, J. Geophys. Res. Biogeosciences, 112, 2007.

Chuine, I. and Cour, P.: Climatic determinants of budburst seasonality in four temperate-zone tree species, New Phytol., 143, 339–349, 1999.

Chuvieco, E. and Martin, M. P.: A simple method for Are growth mapping using AVHRR channel 3 data, Remote Sens., 15, 3141–3146, 1994.

Cochrane, M. A.: Fire science for rainforests, Nature, 421, 913–919, 2003.

Cui, W. and Perera, A. H.: What do we know about forest fire size distribution, and why is this knowledge useful for forest management?, Int. J. Wildland Fire, 17, 234–244, 2008.

Davies, G. M., Legg, C. J., O'hara, R., MacDonald, A. J., and Smith, A. A.: Winter desiccation and rapid changes in the live fuel moisture content of Calluna vulgaris, Plant Ecol. Divers., 3, 289–299, 2010.

Fire Management: https://www.gov.ie/en/publication/01773-fire-management/, last access: 18 November 2021.

Department of Agriculture, Food and the Marine: Prescribed Burning Code of Practice - Ireland, https://www.gov.ie/en/publication/01773-fire-management/, 2021.

European Union: Corine Land Cover (CLC) 2018, Copernicus Land Monitoring Service 2018, 2019a.

Fares, S., Bajocco, S., Salvati, L., Camarretta, N., Dupuy, J.-L., Xanthopoulos, G., Guijarro, M., Madrigal, J., Hernando, C., and Corona, P.: Characterizing potential wildland fire fuel in live vegetation in the Mediterranean region, Ann. For. Sci., 74, 1, 2017.

Feranec, J., Jaffrain, G., Soukup, T., and Hazeu, G.: Determining changes and flows in European landscapes 1990–2000 using CORINE land cover data, Appl. Geogr., 30, 19–35, 2010.

Fernandez-Anez, N., Krasovskiy, A., Müller, M., Vacik, H., Baetens, J., Hukić, E., Kapovic Solomun, M., Atanassova, I., Glushkova, M., and Bogunović, I.: Current wildland fire patterns and challenges in Europe: a synthesis of national perspectives, Air Soil Water Res., 14, 11786221211028184, 2021.

Foresty Commission England: Wildfire Statistics for England 2009-10 to 2016-17, Forestry Commission England, Bristol, 2019b.

Fu, Z., Ciais, P., Bastos, A., Stoy, P. C., Yang, H., Green, J. K., Wang, B., Yu, K., Huang, Y., Knohl, A., Šigut, L., Gharun, M., Cuntz, M., Arriga, N., Roland, M., Peichl, M., Migliavacca, M., Cremonese, E., Varlagin, A., Brümmer, C., Gourlez de la Motte, L., Fares, S., Buchmann, N., El-Madany, T. S.,

Pitacco, A., Vendrame, N., Li, Z., Vincke, C., Magliulo, E., and Koebsch, F.: Sensitivity of gross primary productivity to climatic drivers during the summer drought of 2018 in Europe, Philos. Trans. R. Soc. B Biol. Sci., 375, 20190747, https://doi.org/10.1098/rstb.2019.0747, 2020.

Gazzard, R., McMorrow, J., and Aylen, J.: Wildfire policy and management in England: an evolving response from Fire and Rescue Services, forestry and cross-sector groups, Philos. Trans. R. Soc. B Biol. Sci., 371, 20150341, https://doi.org/10.1098/rstb.2015.0341, 2016.

Gill, A. M., Allan, G., Gill, A. M., and Allan, G.: Large fires, fire effects and the fire-regime concept, Int. J. Wildland Fire, 17, 688–695, https://doi.org/10.1071/WF07145, 2008.

Girden, E..: ANOVA: Repeated measures (No. 84), Sage University Papers Series.

Hantson, S., Pueyo, S., and Chuvieco, E.: Global fire size distribution is driven by human impact and climate, Glob. Ecol. Biogeogr., 24, 77–86, 2015.

Huang, X., and Rein, G.: Downward spread of smouldering peat fire: the role of moisture, density and oxygen supply. International Journal of Wildland Fire, 26(11), 907-918. 2017

Jin, Y., Goulden, M. L., Faivre, N., Veraverbeke, S., Sun, F., Hall, A., Hand, M. S., Hook, S., and Randerson, J. T.: Identification of two distinct fire regimes in Southern California: implications for economic impact and future change, Environ. Res. Lett., 10, 094005, 2015.

Johnston, J. M., Jackson, N., McFayden, C., Ngo Phong, L., Lawrence, B., Davignon, D., Wooster, M. J., van Mierlo, H., Thompson, D. K., and Cantin, A. S.: Development of the User Requirements for the Canadian WildFireSat Satellite Mission, Sensors, 20, 5081, 2020.

de Jong, M. C., Wooster, M. J., Kitchen, K., Manley, C., Gazzard, R., and McCall, F. F.: Calibration and evaluation of the Canadian Forest Fire Weather Index (FWI) System for improved wildland fire danger rating in the United Kingdom, Nat. Hazards Earth Syst. Sci., 16, 1217–1237, https://doi.org/10.5194/nhess-16-1217-2016, 2016.

Keeley, J. E., Pausas, J. G., Rundel, P. W., Bond, W. J., and Bradstock, R. A.: Fire as an evolutionary pressure shaping plant traits, Trends Plant Sci., 16, 406–411, https://doi.org/10.1016/j.tplants.2011.04.002, 2011.

Kitzberger, T., Perry, G. L. W., Paritsis, J., Gowda, J. H., Tepley, A. J., Holz, A., and Veblen, T. T.: Fire–vegetation feedbacks and alternative states: common mechanisms of temperate forest vulnerability to fire in southern South America and New Zealand, N. Z. J. Bot., 54, 247–272, 2016.

Krawchuk, M. A., Moritz, M. A., Parisien, M.-A., Dorn, J. V., and Hayhoe, K.: Global Pyrogeography: the Current and Future Distribution of Wildfire, PLOS ONE, 4, e5102, https://doi.org/10.1371/journal.pone.0005102, 2009.

Le Houérou, H. N.: Fire and vegetation in the Mediterranean Basin, FAO, 1973.

Linn, R. R. and Cunningham, P.: Numerical simulations of grass fires using a coupled atmosphere–fire

model: basic fire behavior and dependence on wind speed, J. Geophys. Res. Atmospheres, 110, 2005.

Liu, X., He, B., Quan, X., Yebra, M., Qiu, S., Yin, C., Liao, Z., and Zhang, H.: Near Real-Time Extracting Wildfire Spread Rate from Himawari-8 Satellite Data, Remote Sens., 10, 1654, https://doi.org/10.3390/rs10101654, 2018.

Loboda, T. V. and Csiszar, I. A.: Reconstruction of fire spread within wildland fire events in Northern Eurasia from the MODIS active fire product, Glob. Planet. Change, 56, 258–273, https://doi.org/10.1016/j.gloplacha.2006.07.015, 2007.

Lung, T., Lavalle, C., Hiederer, R., Dosio, A., and Bouwer, L. M.: A multi-hazard regional level impact assessment for Europe combining indicators of climatic and non-climatic change, Glob. Environ. Change, 23, 522–536, https://doi.org/10.1016/j.gloenvcha.2012.11.009, 2013.

McWethy, D. B., Higuera, P. E., Whitlock, C., Veblen, T. T., Bowman, D. M. J. S., Cary, G. J., Haberle, S. G., Keane, R. E., Maxwell, B. D., McGlone, M. S., Perry, G. L. W., Wilmshurst, J. M., Holz, A., and Tepley, A. J.: A conceptual framework for predicting temperate ecosystem sensitivity to human impacts on fire regimes, Glob. Ecol. Biogeogr., 22, 900–912, https://doi.org/10.1111/geb.12038, 2013.

Miller, R. G., Tangney, R., Enright, N. J., Fontaine, J. B., Merritt, D. J., Ooi, M. K., Ruthrof, K. X., and Miller, B. P.: Mechanisms of fire seasonality effects on plant populations, Trends Ecol. Evol., 34, 1104–1117, 2019.

Moreira, F., Vaz, P., Catry, F., and Silva, J. S.: Regional variations in wildfire susceptibility of land-cover types in Portugal: implications for landscape management to minimize fire hazard, Int. J. Wildland Fire, 18, 563–574, 2009.

Moreno, M. V., Chuvieco, E.: Characterising fire regimes in Spain from fire statistics, Int. J. Wildland Fire, 22, 296-305, 2013.

Moritz, M. A., Parisien, M.-A., Batllori, E., Krawchuk, M. A., Dorn, J. V., Ganz, D. J., and Hayhoe, K.: Climate change and disruptions to global fire activity, Ecosphere, 3, art49, https://doi.org/10.1890/ES11-00345.1, 2012.

Heather and grass burning: rules and applying for a licence: https://www.gov.uk/guidance/heather-and-grass-burning-apply-for-a-licence, last access: 19 November 2021.

Guidance - The Muirburn Code: https://www.nature.scot/doc/guidance-muirburn-code, last access: 19 November 2021.

Oliva, P. and Schroeder, W.: Assessment of VIIRS 375m active fire detection product for direct burned area mapping, Remote Sens. Environ., 160, 144–155, https://doi.org/10.1016/j.rse.2015.01.010, 2015.

Parsons, R., Jolly, W. M., Hoffman, C., and Ottmar, R.: The role of fuels in extreme fire behavior, Synth. Knowl. Extreme Fire Behav., 55, 2016.

Pausas, J. G. and Paula, S.: Fuel shapes the fire–climate relationship: evidence from Mediterranean

ecosystems, Glob. Ecol. Biogeogr., 21, 1074–1082, 2012.

Rein, G., and Huang, X.: Smouldering wildfires in peatlands, forests and the arctic: Challenges and perspectives. Current Opinion in Environmental Science & Health, 24, 100296. 2021

de Rigo, D., Libertà, G., Houston Durrant, T., Vivancos, T. A., San-Miguel-Ayanz, J., and Union, P. O. of the E.: Forest fire danger extremes in Europe under climate change: variability and uncertainty, Publications Office of the European Union, https://doi.org/10.2760/13180, 2017.

Sá, A. C. L., Benali, A., Fernandes, P. M., Pinto, R. M. S., Trigo, R. M., Salis, M., Russo, A., Jerez, S., Soares, P. M. M., Schroeder, W., and Pereira, J. M. C.: Evaluating fire growth simulations using satellite active fire data, Remote Sens. Environ., 190, 302–317, https://doi.org/10.1016/j.rse.2016.12.023, 2017.

San-Miguel-Ayanz, J., Durrant, T., Boca, R., Libertà, G., Branco, A., de Rigo, D., Ferrari, D., Maianti, P., Artes, V., Oom, D., Pfeiffer, H., Nuijten, D., and Leray, T.: JRC Technical Report - Forest Fires in Europe, Middle East and North Africa 2018, Publ. Off. Eur. Union, 164, https://doi.org/10.2760/561734, 2019.

San-Miguel-Ayanz, J., Durrant, T., Boca, R., Libertà, G., Branco, A., de Rigo, D., Ferrari, D., Maianti, P., Artes, V., Oom, D., Pfeiffer, H., Grecchi, R., Nuijten, D., Onida, M., and Loffler, P.: JRC Technical Report - Forest Fires in Europe, Middle East and North Africa 2020, Publ. Off. Eur. Union, 174, https://doi.org/10.27760/059331, 2021.

Santoso, M. A., Christensen, E. G., Yang, J., and Rein, G.: Review of the transition from smouldering to flaming combustion in wildfires, Front. Mech. Eng., 5, 49, 2019.

Schroeder, W., Oliva, P., Giglio, L., and Csiszar, I. A.: The New VIIRS 375 m active fire detection data product: Algorithm description and initial assessment, Remote Sens. Environ., 143, 85–96, 2014.

Stoof, C. R., Tapia, V. M., Marcotte, A. L., Stoorvogel, J. J., and Castellnou Ribau, M.: Relatie tussen natuurbeheer en brandveiligheid in de Deurnese Peel : onderzoek naar aanleiding van de brand in de Deurnese Peel van 20 april 2020, Wageningen University & Research, Wageningen, https://doi.org/10.18174/533574, 2020.

Sundseth, K., Houston, J., and Eriksson, M.: Natura 2000 in the Atlantic Region, Office for Official Publications of the European Communities, LU, 12 pp., 2009.

Tedim, F., Xanthopoulos, G., and Leone, V.: Forest fires in Europe: Facts and challenges, in: Wildfire hazards, risks and disasters, Elsevier, 77–99, 2015.

Vaillant, N. M., Fites-Kaufman, J., Reiner, A. L., Noonan-Wright, E. K., and Dailey, S. N.: Effect of Fuel Treatments on Fuels and Potential Fire Behavior in California, USA, National Forests, Fire Ecol., 5, 14–29, https://doi.org/10.4996/fireecology.0502014, 2009.

Veraverbeke, S., Sedano, F., Hook, S. J., Randerson, J. T., Jin, Y., Rogers, B. M., Veraverbeke, S.,

Sedano, F., Hook, S. J., Randerson, J. T., Jin, Y., and Rogers, B. M.: Mapping the daily progression of large wildland fires using MODIS active fire data, Int. J. Wildland Fire, 23, 655–667, https://doi.org/10.1071/WF13015, 2014.

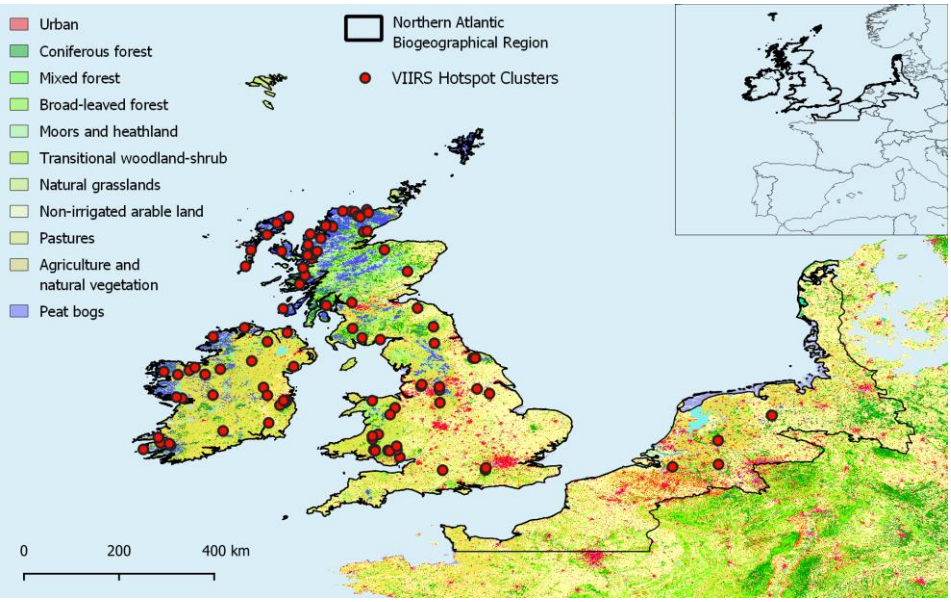

***Figure 1. Study area of northwest Europe, encompassing the United Kingdom, Ireland, the Netherlands, Belgium, Denmark, northern France and northwestern Deutschland within the northern Atlantic biogeographical region above 49th parallel (Sundseth et al., 2009). Locations of the fire hotspot clusters from VIIRS 375 m active fire product (*VNP14IMGTDL_NRT; https://firms.modaps.eosdis.nasa.gov/download/*) derived from 344,000 hotspot detections from January 2012 through June 2020. Land cover map of the study area (*Copernicus Land Monitoring Service's Corine Land Cover Map 2018 (2019a)**

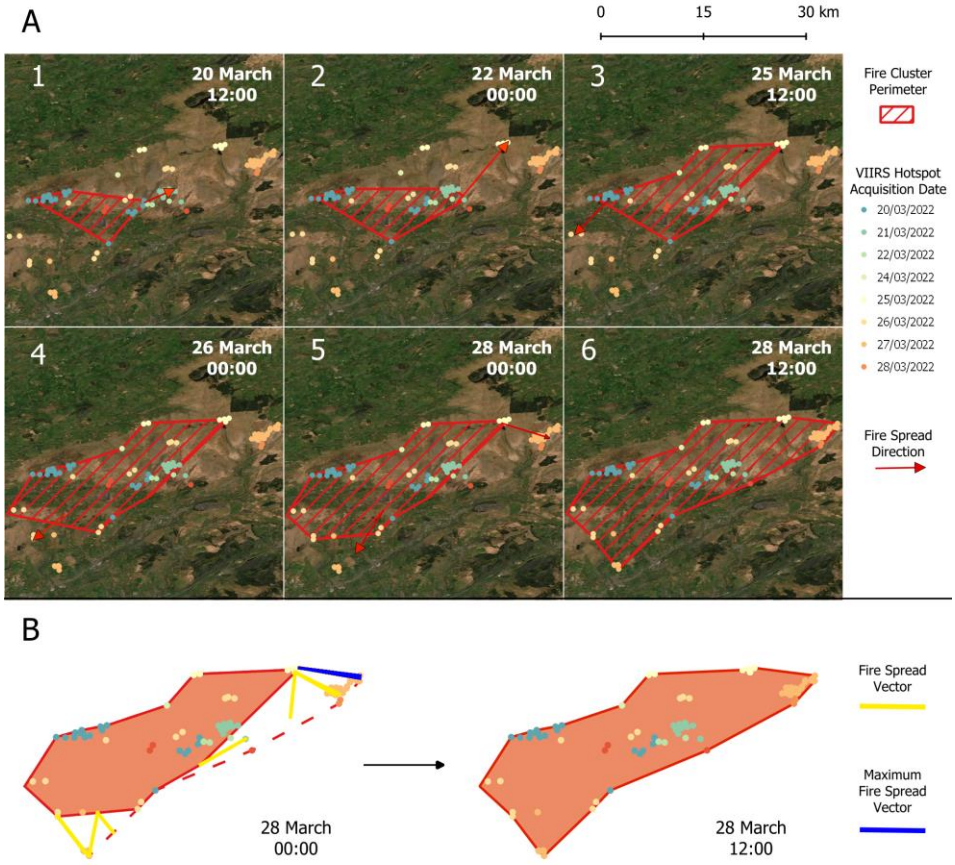

Figure 2. Multipolygons and spread vectors for the Mynydd Mawr fire in Wales (March 20, 2022), representing the methodology used to delineate fire perimeters and Rate of Spread (ROS) vectors. A) Scheme of the fire growth in several time steps throughout the fire duration delineated using the VIIRS hotspots (VIIRS 375 m active fire product at each satellite overpass (VNP14IMGTDL_NRT; https://firms.modaps.eosdis.nasa.gov/download/). Red arrows represent the main fire spread direction. B) Real ROS vectors (yellow lines) and perimeters generated (orange polygons). For each time step, the maximum ROS vector is selected for further analyses (blue lines).

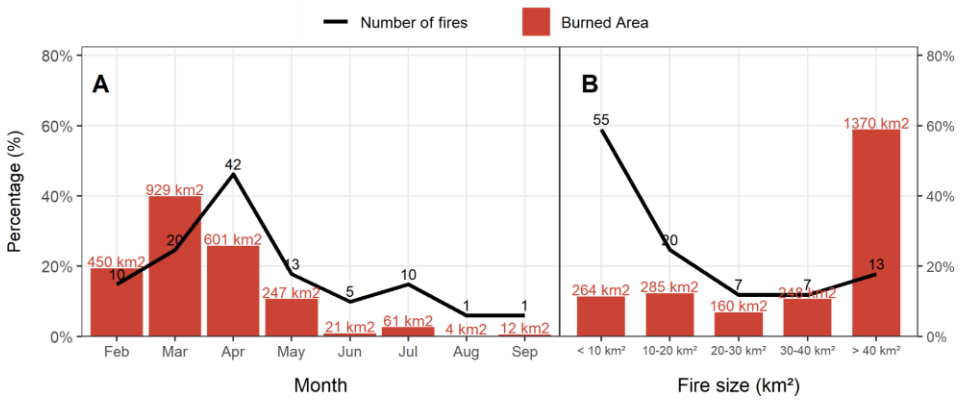

Figure 3: Burned area percentages for Northwest Europe calculated a) monthly and b) according to size distribution at the time the fire ended . Notice that this burned area may not be the same as that detected by other remotely sensed burned area products, or delineated in the GIS systems maintained by fire managers due to the spatial resolution limitations of the active fire product used in this work (*VNP14IMGTDL_NRT; https://firms.modaps.eosdis.nasa.gov/download/*).

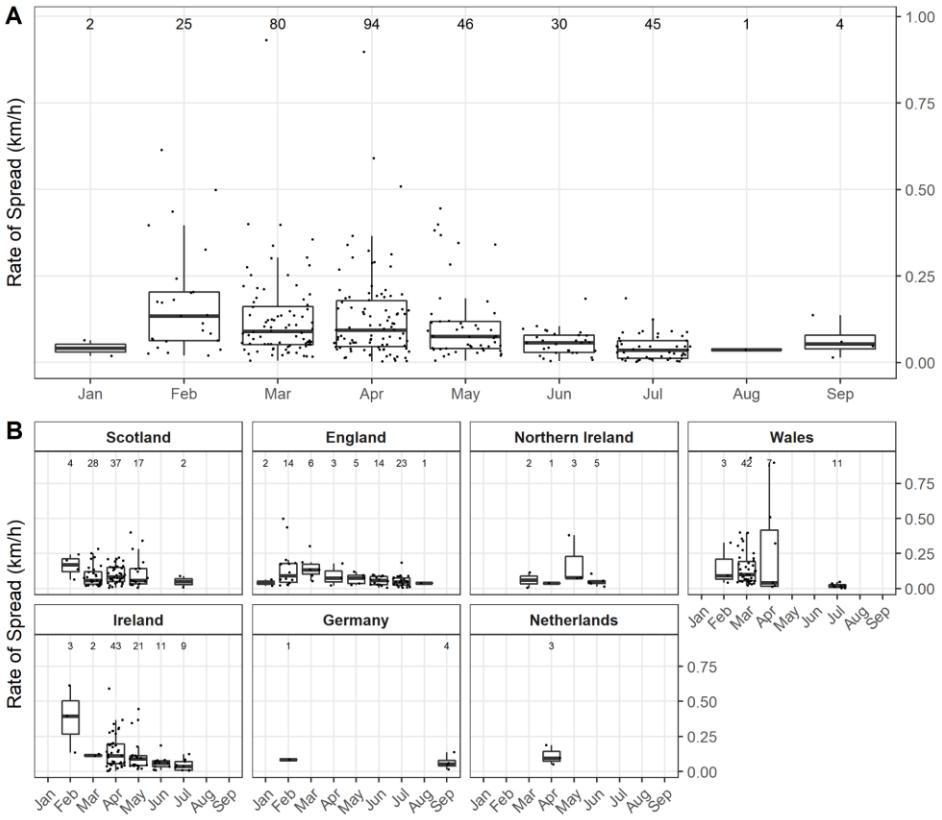

Figure 4: Rate of spread for northwest Europe from 2012–2020 calculated monthly A) for the northwest European area (northern Atlantic biogeographical region) and B) per country. Points represent sample size and it is also indicated as numbers on top of each boxplot. Fires were not detected for months not represented in the figure.

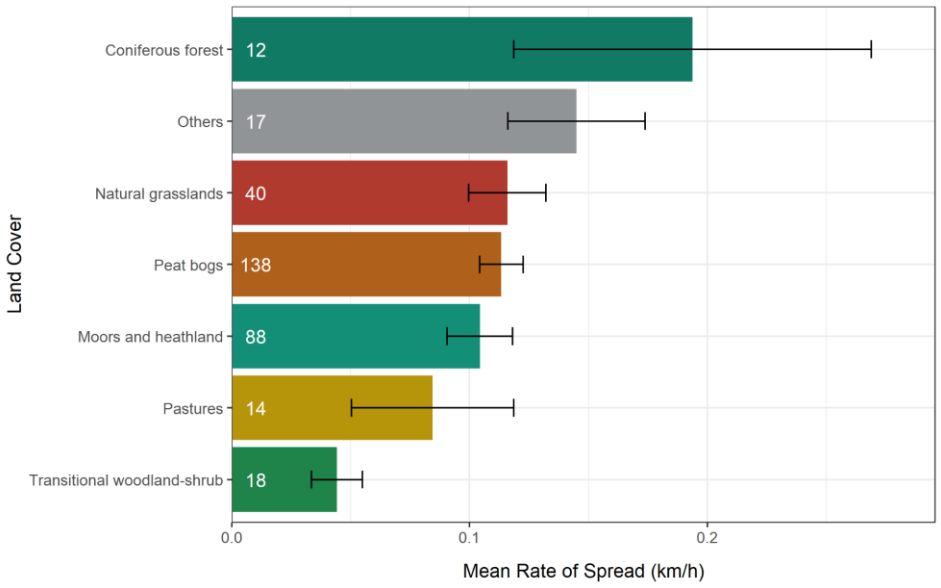

Figure 5: Rate of Spread across various represented land cover types in northwest Europe. The category "others" includes other land cover types with low representation (less than 10 maximum spread vectors by category). Number of observations pointed in numbers for each type.

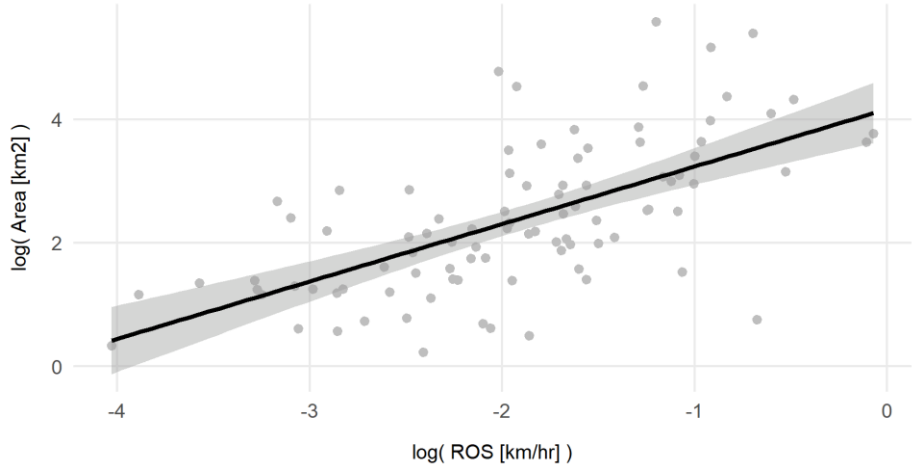

Figure 6 : Linear regression model for log-transformed variables indicating a positive relationship between maximum rate of spread (ROS) vectors and final burned area for each fire.